

ARTICLE

Open Access

Autophagic cell death participates in POMC-induced melanoma suppression

Jian-Ching Wu^{1,2}, Han-En Tsai³, Guei-Sheung Liu^{4,5}, Chieh-Shan Wu⁶ and Ming-Hong Tai^{1,7,8}

Abstract

Hypoxia in tumors is known to trigger the pro-survival pathways such as autophagy. Systemic proopiomelanocortin (POMC) gene therapy suppresses melanoma through apoptosis induction and neovascularization blockage. In this study, we investigated the crosstalk between autophagic and apoptotic signaling in POMC-mediated melanoma suppression. By histological and immunoblot analysis, it was shown that POMC-treated melanoma tissues exhibited the prominent LC3 immunostaining, which was correlated with reduced CD31-positive tumor vascularization. Such autophagy induction could be recapitulated in melanoma cells receiving POMC gene delivery and hypoxia-mimicking agent cobalt chloride (CoCl₂). We then utilized the POMC-derived peptide α -MSH with CoCl₂ to elicit the autophagy as well as apoptosis in cultured melanoma cells. To delineate the role of autophagy during cell death, application of autophagy-inducer rapamycin enhanced, whereas autophagy inhibitor 3-MA attenuated, the α -MSH-induced apoptosis in melanoma cells. Genetic silencing of ATG5, an autophagy regulator, by RNA interference perturbed the α -MSH-induced apoptosis in melanoma cells. Finally, it was delineated that α -MSH stimulated the HIF-1 α signaling as well as the expression of BNIP3/BNIP3L, thereby promoting the autophagy and apoptosis in melanoma cells. Therefore, the present study unveiled a unique function of autophagy in promoting cell death during POMC-mediated melanoma suppression via α -MSH/HIF-1 α /BNIP3/BNIP3L signaling pathway.

Introduction

Hypoxia is a common characteristic of pathological features presenting in solid tumors and is associated with a poor outcome. Generally, tumor cells are well adapted to moderate hypoxia by inducing several genes involved in angiogenesis, glycolysis, glucose uptake and metastasis¹. However, in complex conditions such as glucose deprivation or acidosis, hypoxia is also capable of inducing apoptosis and autophagic cell death through a hypoxia-inducible factor-1 (HIF-1)-independent manner or reactive oxygen species (ROS) stimuli^{2–5}. Recent studies have

shown that hypoxia-induced autophagy and apoptosis are crosstalk from many common upstream pathways, indicating that they can regulate each other^{6,7}. Although the relationship between autophagy and apoptosis has been known for rather complex during hypoxia, the role of autophagy and molecular regulatory mechanisms between autophagy and apoptosis are not clearly understood.

Autophagy is a self-degradative process for the cellular stress adaptation response that maintains cell homeostasis and protection⁸. Once activated, the autophagic process initially requires the dissociated Beclin-1 from Bcl-2 or Bcl-X_L binds to class III phosphatidylinositol 3-kinase (PIK3C3 or Vps34) that forms an initiation complex and recruits autophagy-related protein 7 (ATG7) to the developing phagopore. Autophagosomal elongation then recruits two ubiquitin-like conjugation systems, ATG12-ATG5 and subsequent phosphatidylethanolamine conjugated form of the microtubule-associated protein light

Correspondence: Chieh-Shan Wu (dermawu@vghks.gov.tw) or Ming-Hong Tai (minghongtai@gmail.com)

¹Doctoral Degree Program in Marine Biotechnology, National Sun Yat-sen University, 70 Lien-Hai Road, Kaohsiung 80424, Taiwan

²Doctoral Degree Program in Marine Biotechnology, Academia Sinica, 128 Academia Road, Section 2, Nankang, Taipei 11529, Taiwan

Full list of author information is available at the end of the article.

These authors contributed equally: Jian-Ching Wu, Han-En Tsai

Edited by R. Aqeilan

© 2018 The Author(s).



Open Access This article is licensed under a Creative Commons Attribution 4.0 International License, which permits use, sharing, adaptation, distribution and reproduction in any medium or format, as long as you give appropriate credit to the original author(s) and the source, provide a link to the Creative Commons license, and indicate if changes were made. The images or other third party material in this article are included in the article's Creative Commons license, unless indicated otherwise in a credit line to the material. If material is not included in the article's Creative Commons license and your intended use is not permitted by statutory regulation or exceeds the permitted use, you will need to obtain permission directly from the copyright holder. To view a copy of this license, visit <http://creativecommons.org/licenses/by/4.0/>.

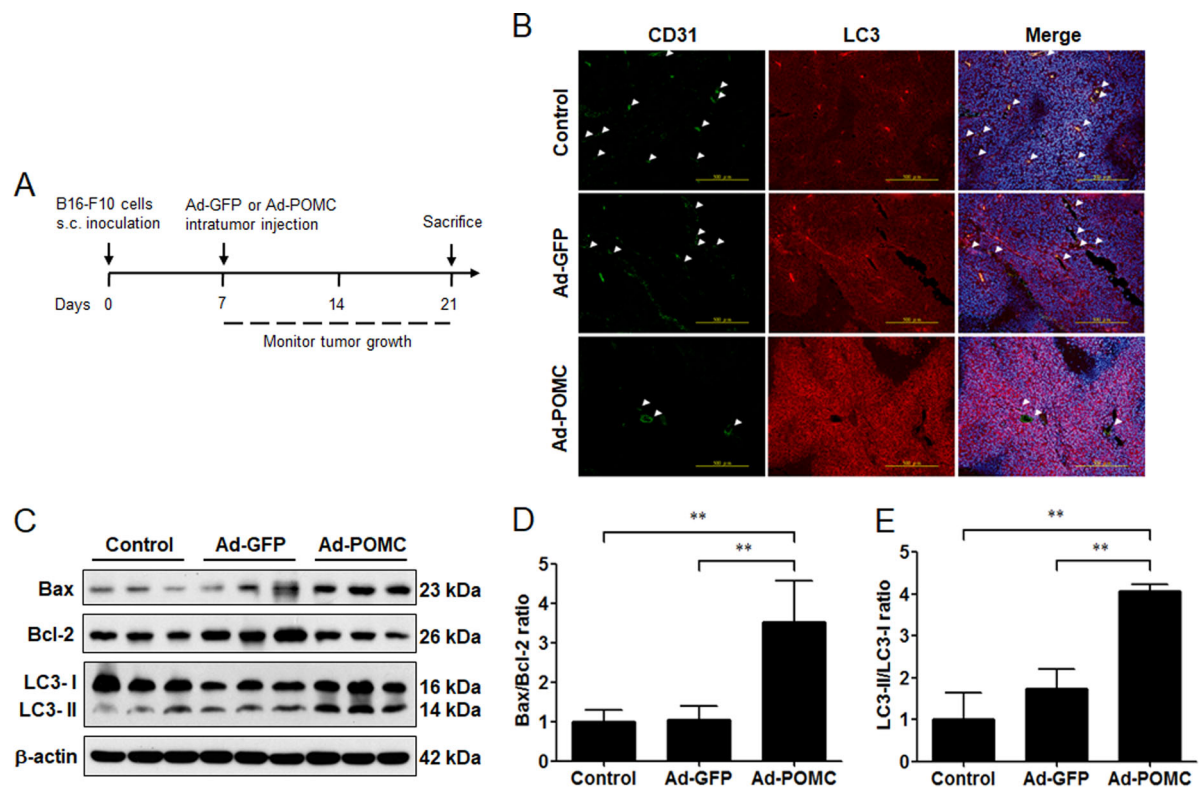


Fig. 1 Elevated autophagic activity in Ad-POMC-treated melanoma. **a** After subcutaneous inoculation of B16-F10 cells in C57BL/6 mice for 7 days (5×10^5 cells in 0.1 ml of PBS per mice), mice were administered adenovirus vector carrying GFP or POMC gene (1×10^9 pfu in 0.1 of PBS) by intratumor injection. The melanoma tissues were dissected for the following experimental analysis at the indicated end point. **b** Autophagic LC3 (red) and CD31 (green) co-staining in Ad-POMC-treated melanoma tissues. The number of CD31-positive microvessel was reduced in Ad-POMC-treated melanoma tissues (white arrowheads). Cell nucleus was stained by DAPI (blue). Scale bar, 500 μ m. **c** Immunoblot analysis of LC3 expression in melanoma tissues. The protein extracts from different groups of melanoma tissues ($n = 3$ per group) were analyzed by immunoblot analysis. β -Actin was used as internal control. **d, e** The ratio of Bax/Bcl-2 and LC3-II/LC3-I was quantified by relative intensities of protein bands. $**p < 0.01$. Thus POMC gene therapy elevated autophagy and Bax/Bcl-2 ratio in melanoma tissues

chain 3 (LC3-II)⁹. Autophagy not only protects against diverse pathologies, such as infections, neurodegeneration, aging, and inflammation^{10,11} but also modulates CD4⁺ T cell population and enhancement of adaptive immune responses¹². Moreover, accumulating studies point to the dual role of autophagy in tumor microenvironment: one aspect is on maintaining tumor cells survival and contributing to tumor progression, and the other one is reversely to promote cancer cell death in some cases^{13–16}. For example, when tumor cells exposed to double stresses such as hypoxia and ATP deprivation situation, inducible autophagy can lead to the mitochondrial dysfunction and cell death by HIF-1 α -mediated Bcl-2 gene families, such as *BNIP3* (Bcl-2 adenovirus E1a nineteen kilodalton interacting protein 3) and *BNIP3L* (Bcl-2 adenovirus E1a nineteen kilodalton interacting protein 3-like)^{17–19}. Therefore, targeting autophagy for cancer therapy may present selectivity dependent on cell adaptation in tumor microenvironment.

Proopiomelanocortin (POMC) is a precursor of multiple peptide hormones, which is expressed in hypothalamic neurons and melanocytes and keratinocytes. POMC products (the adrenocorticotrophic hormone, melanocyte-stimulating hormones [MSHs], and β -endorphin) manage pleiotropic functions, including pigmentation, adrenocortical function, regulation of energy homeostasis, and immunity modulation^{20–23}. Our previous studies showed that utilizing the POMC gene carrying by adenovirus is efficient way for Lewis lung carcinoma and melanoma suppression in vivo, we then characterized that POMC-derived peptide α -MSH not only inhibits the colony-forming capacity and invasion of melanoma cells^{24–26} but also retards the tube formation and migration in endothelial cells^{27,28}. In addition, α -MSH can mimic POMC-induced apoptosis during hypoxia by increasing ROS generation²⁹. However, the mechanisms of POMC-induced apoptosis in melanoma cells under hypoxic condition is still not enough

comprehension. This study aimed to reveal how autophagy and apoptosis work together in response to double stress (hypoxia and α -MSH) stimuli in melanoma cells.

Results

POMC gene therapy elicits autophagy in melanoma in vivo

Because it is known that POMC gene therapy induces apoptosis in melanoma via α -MSH during hypoxic challenge²⁹, we would like to elucidate whether autophagy also occurred and participated in POMC-induced melanoma suppression. To address this question, after executing the primary melanoma model as shown in Fig. 1a, the tumor tissues were fixed and sectioned for histological analysis. By immunofluorescence staining, it was revealed that a strong LC3 staining was observed in adenovirus (Ad)-POMC-infected tumors compared with Ad-green fluorescent protein (GFP)-infected tumors, and it was correlated with low density of CD31-positive microvessels, implying that POMC-induced autophagy might occur under hypoxic stress (Fig. 1b). Moreover, immunoblot analysis revealed that the protein levels of Bax and LC3-II in Ad-POMC-infected tumor tissues were higher than that in Ad-GFP-infected group (Fig. 1c). Quantification analysis further indicated that the Bax/Bcl-2 ratio and LC3-II/LC3-I conversion were significantly increased in Ad-POMC-infected melanoma tissues (Fig. 1d, e). These results indicated that POMC gene therapy induces the autophagic flux in melanoma.

POMC gene delivery promotes the autophagic formation in B16-F10 melanoma cells during hypoxia

Subsequently, we investigated whether POMC gene delivery could enhance the autophagy in B16-F10 melanoma cells. By GFP-LC3 puncta formation assay, it was found that POMC gene delivery marginally promoted the GFP-LC3 puncta spots in melanoma cells under normoxic condition (Fig. 2a, b). Strikingly, POMC gene delivery significantly stimulated the GFP-LC3 puncta formation in melanoma cells during hypoxia by cobalt chloride (CoCl₂; Fig. 2a, b). To confirm this finding, immunoblot analysis showed that POMC gene delivery reversed the hypoxia-induced Beclin 1 downregulation and increased LC3-I and -II protein levels under hypoxic challenge, although it did not affect the LC3-II/LC3-I conversion, suggesting that POMC gene delivery not only stimulated the autophagic activity but also enhanced the total protein level of LC3 (Fig. 3c). These results suggested that autophagy could be recapitulated in B16-F10 melanoma cells by combined POMC overexpression with hypoxia-inducing agent.

α -MSH evoked the autophagy in B16-F10 melanoma cells during hypoxia

α -MSH has been demonstrated as the primary neuropeptide responsible for the apoptosis-inducing

as well as the anti-neoplastic function of POMC gene therapy in melanoma^{24,27,29}. Thus we examined whether α -MSH application also modulated the autophagy in melanoma cells. By using GFP-LC3 puncta formation assay, it was shown that α -MSH prominently increased the GFP-LC3 puncta spots in CoCl₂-treated B16-F10 melanoma cells (Fig. 3a, b) but had no effect on autophagy in normoxic condition. Consistently, immunoblot analysis revealed that α -MSH enhanced LC3-II protein expression and reversed hypoxia-induced Beclin 1 suppression during hypoxia (Fig. 3c). These findings suggested that α -MSH was sufficient to mimic the POMC-mediated autophagy regulation in melanoma cells.

Autophagy inhibitor 3-methyladenine (3-MA) suppresses, while autophagy-inducer rapamycin enhances, the α -MSH-induced apoptosis of melanoma cells during hypoxia

Because α -MSH simultaneously evokes autophagy and apoptosis in melanoma cells during hypoxia, it is pivotal to elucidate the role of autophagy on α -MSH-induced apoptosis in melanoma cells. By flow cytometric analysis, it was shown that application of autophagy inhibitor 3-MA potently attenuated the α -MSH-induced apoptosis in B16-F10 melanoma cells during hypoxia (from 14.19 to 11.23%). On the contrary, treatment with autophagy-inducer rapamycin significantly enhanced the α -MSH-induced apoptosis in melanoma cells (from 14.19 to 17.98%; Fig. 4a). Immunoblot analysis also revealed that 3-MA retarded α -MSH-induced Beclin 1, ATG5, and cleaved caspase-3 expression levels, while rapamycin was prominent to elevate the level of cleaved caspase-3 both in α -MSH treatment under hypoxic condition and CoCl₂ only group (Fig. 4b).

ATG5 silencing attenuated the α -MSH-induced apoptosis

Since ATG5 is an important regulator of autophagy³⁰, we investigated the effect of ATG5 knockdown on α -MSH-induced apoptosis. By RNA interference technique, it was demonstrated that shATG5 #1 and #2 plasmids' transfection were workable to the basal ATG5 mRNA and protein expression levels in B16-F10 melanoma cells (Fig. 5a). As expected, silencing ATG5 had a higher proportion of apoptosis in the control and CoCl₂ groups, but no significant increase under α -MSH and hypoxia double stresses compared to CoCl₂ only groups (Fig. 5b). Moreover, immunoblot analysis also revealed that silencing ATG5 was partially to diminish α -MSH-induced cleaved caspase-3 and LC3-II expression levels during hypoxia (Fig. 5c). Therefore, these results proposed that α -MSH-induced autophagy was prone to boosting apoptosis rather than assist the cell survival during hypoxia.

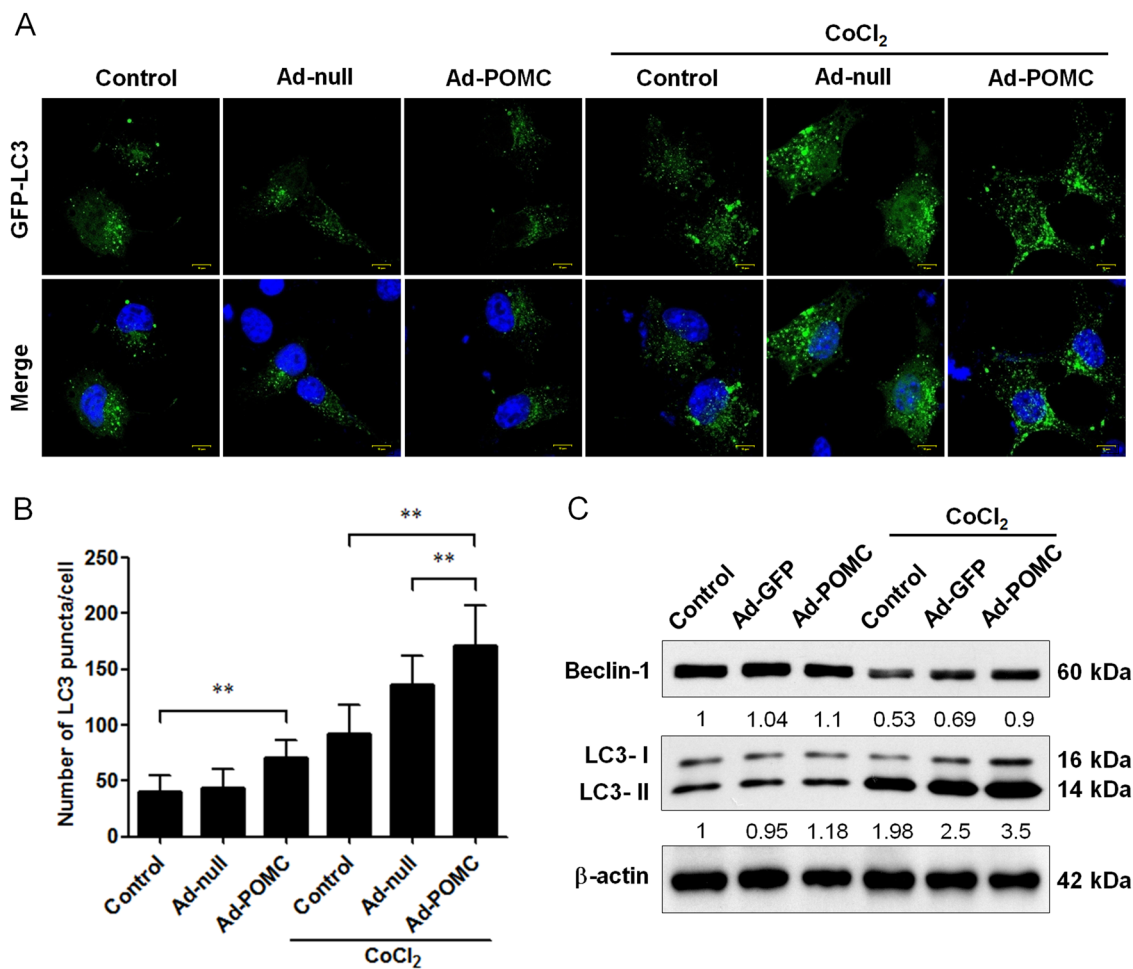


Fig. 2 Effect of POMC gene delivery on autophagy in melanoma cells during hypoxia. **a** After transfection with GFP-LC3 plasmid for 24 h, cells were infected with adenovirus vectors at MOI of 1000 for 24 h and then incubated in the presence or absence of CoCl₂ (100 μ M) for another 24 h. POMC gene delivery increased GFP-LC3 spots in cells exposed to hypoxic condition. **b** The number of GFP-LC3 spots was monitored by confocal microscopy and quantified. Scale bar, 10 μ m. **c** Cell lysates were analyzed by immunoblot with the indicated antibodies. β -Actin was used as an internal control for loading and transfer. ** p < 0.01. Hence, POMC gene delivery enhanced autophagic activities in B16-F10 melanoma cells during hypoxia

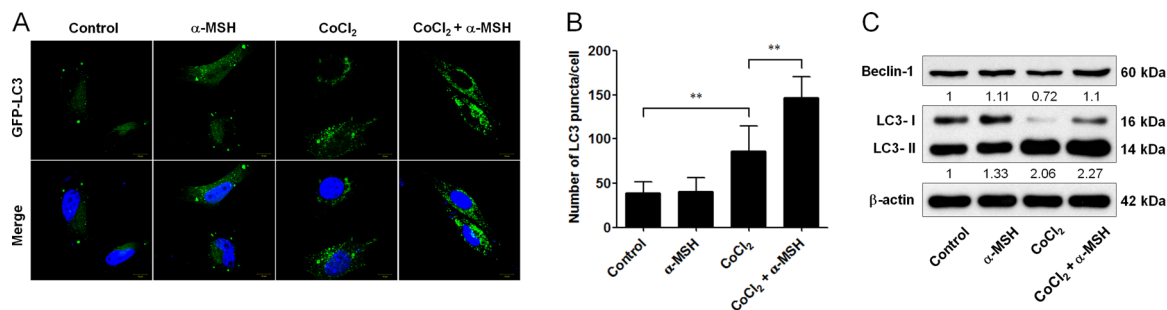


Fig. 3 Effect of α -MSH on autophagy in B16-F10 melanoma cells during hypoxia. **a** α -MSH increased GFP-LC3 spots in cells exposed to hypoxic condition. **b** The number of GFP-LC3 spots was observed by confocal microscopy and quantified. Scale bar, 10 μ m. **c** α -MSH enhanced the protein level of Beclin 1 and LC3-II in B16-F10 melanoma cells during hypoxia. ** p < 0.01. α -MSH enhanced autophagic activities in B16-F10 melanoma cells during hypoxia

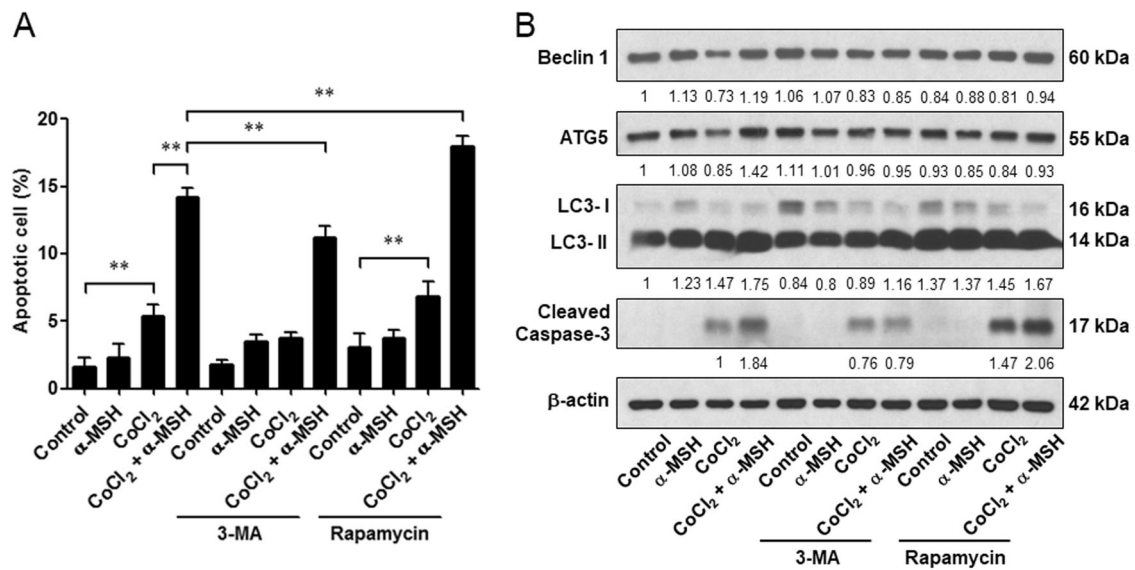


Fig. 4 Effect of autophagy modulators on α -MSH-induced apoptosis in B16-F10 melanoma cells during hypoxia. After treatment with α -MSH for 24 h, cells were incubated with 3-MA or rapamycin in the presence of CoCl_2 challenge for another 24 h. **a** Cell lysates were subjected to immunoblot with the indicated antibodies. β -Actin was used as an internal control for loading and transfer. **b** The population of apoptotic cells was analyzed by flow cytometry and qualified as mean \pm SD from triplicate experiments. $**p < 0.01$. Autophagy inhibitor 3-MA decreased, whereas autophagy-inducer rapamycin increased, the α -MSH-induced apoptosis in B16-F10 melanoma cells during hypoxia

α -MSH augmented HIF-1 α signaling to regulate Bcl-2 family gene expression levels in melanoma cells

Since HIF-1 α /BNIP3/Beclin 1 is considered a general autophagy signaling pathway³¹, we thus investigated whether α -MSH-induced autophagy was via HIF-1 α activation. By quantitative real-time PCR analysis, it was shown that α -MSH significantly augmented HIF-1 α mRNA expression in B16-F10 melanoma cells during hypoxia compared with the CoCl_2 only group, although the mRNA level of HIF-1 α was only slight increased in α -MSH-treated cells in normoxia (Fig. 6a). Moreover, immunoblot and luciferase reporter assays have shown that α -MSH elevated the HIF-1 α -driven luciferase activity and protein levels in both normoxia and hypoxia (Fig. 6b, c). The similar results also were obtained by POMC gene delivery in B16-F10 melanoma cells (Supplementary 1A-C). Because of the Bcl-2 family such as BNIP3 and BNIP3L were triggered by HIF-1 α in autophagic process, we next evaluated whether α -MSH modulated the Bcl-2 family gene expression in melanoma cells during hypoxia. As expected, by quantitative real-time PCR analysis, it was demonstrated that α -MSH significantly increased the gene expression of BNIP3 and BNIP3L in B16-F10 melanoma cells exposed to hypoxic condition (Fig. 6d). Together, these results suggested that α -MSH-induced autophagy in hypoxia was via HIF-1 α -mediated signaling pathway.

HIF-1 α silencing ameliorated the α -MSH-induced apoptosis in melanoma cells during hypoxia

To investigate whether knockdown of HIF-1 α could affect α -MSH-induced apoptosis in B16-F10 melanoma cells during hypoxia, HIF-1 α short hairpin RNA (shRNA) plasmids were exploited to execute the following in vitro study analysis. By immunoblot and quantitative real-time PCR analysis, it was demonstrated that both of HIF-1 α shRNA #1 and #2 transfection significantly attenuated the basal HIF-1 α mRNA and protein expression levels (Fig. 7a). Moreover, knockdown of HIF-1 α by shRNA was efficient to retard α -MSH-induced BNIP3 and BNIP3L gene expression during hypoxia (Fig. 7b, c). More importantly, α -MSH-induced LC3-II and cleaved caspase-3 were partially abrogated in B16-F10 melanoma cells transfected with HIF-1 α shRNA during hypoxia (Fig. 7d). Flow cytometric analysis also demonstrated that silencing HIF-1 α did not elevate the proportion of α -MSH-induced apoptosis, contrarily no statistical difference was observed between α -MSH and CoCl_2 double stresses and CoCl_2 only groups (Fig. 7e). In summary, we herewith propose that α -MSH-induced autophagy partially contributed to cell apoptosis by HIF-1 α /BNIP3/BNIP3L signaling pathway.

Discussion

This study has first demonstrated that POMC gene therapy simultaneously induces two different types of cell

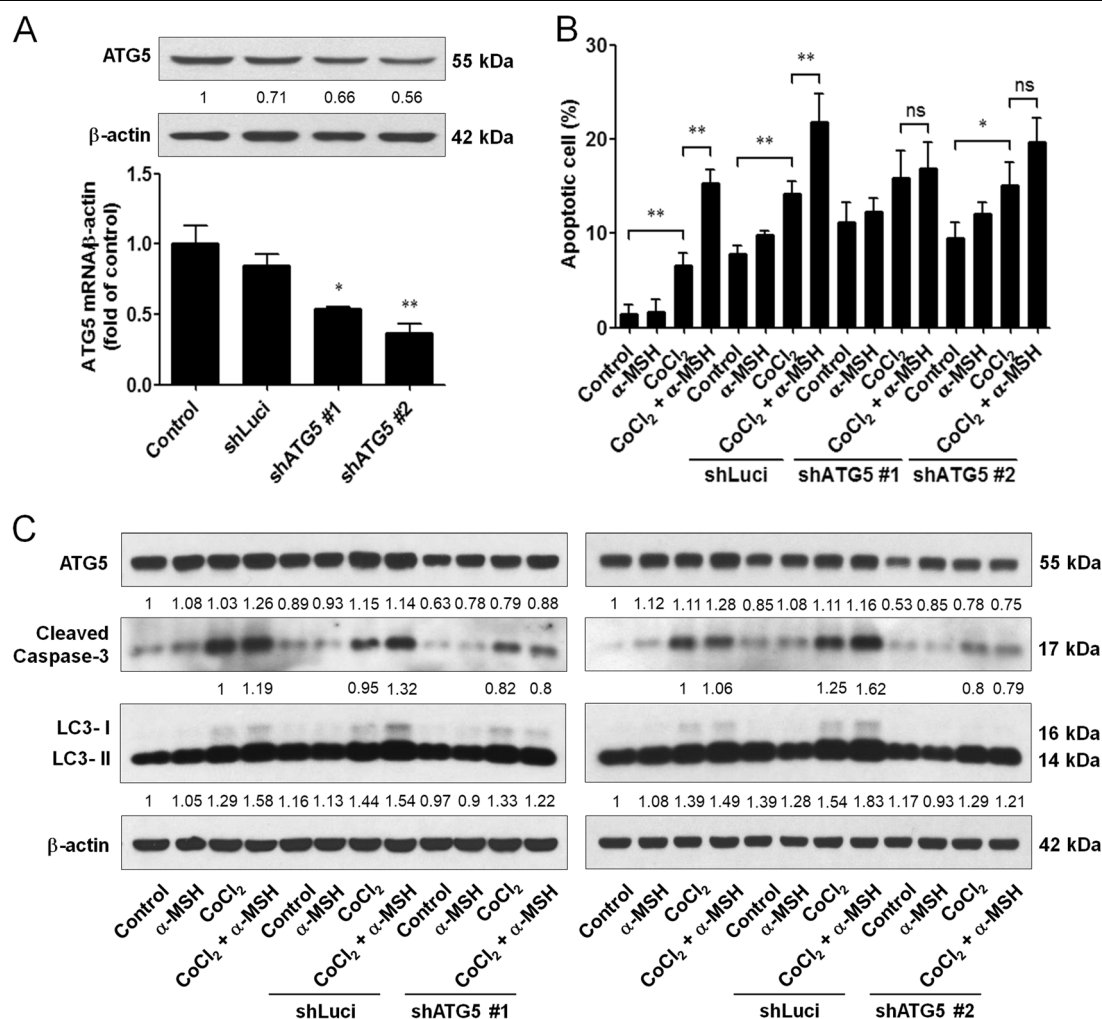


Fig. 5 Effect of ATG5 knockdown on α -MSH-induced apoptosis in B16-F10 melanoma cells during hypoxia. **a** Cells were transfected with shLuci or shATG5 plasmids for 48 h before harvest. ATG5 shRNA reduced the basal ATG5 mRNA and protein expression levels. **b** Silencing ATG5 expression retarded α -MSH-induced apoptosis during hypoxia compared to the shLuci group. **c** Cell lysates were subjected to immunoblot with the indicated antibodies. β -Actin was used as an internal control for loading and transfer. * $p < 0.05$, ** $p < 0.01$. Downregulation of ATG5 attenuated the α -MSH-induced apoptosis in B16-F10 melanoma cells during hypoxia

death: autophagy and apoptosis in melanoma in vivo. This was further validated by cell culture studies, in which POMC gene delivery elevated LC3-positive autophagosome formation in melanoma cells under hypoxia. We subsequently delineated that the POMC-derived α -MSH was sufficient to evoke the autophagy as well as apoptosis in melanoma cells in the presence of CoCl₂. Interestingly, pharmaceutical intervention studies using autophagy modulators reveal that the α -MSH-evoked autophagy participates in the α -MSH-induced cell death rather than protection against environmental stress. This notion was later supported by ATG5 knockdown studies. Finally, we delineated that α -MSH augmented the HIF-1 α signaling during hypoxia, which elevated the expression of downstream Bcl-2 family genes (including BNIP3 and BNIP3L)

to elicit the activation of both autophagic and apoptotic cell death. Moreover, HIF-1 α knockdown retarded the α -MSH-induced autophagosome formation and apoptosis in melanoma cells, implicating the pivotal role of HIF-1 α activation in α -MSH-induced cell death. Therefore, the present study unveils that POMC therapy induces the activation of autophagic and apoptotic cell death pathways in melanoma cells through α -MSH/HIF-1 α /BNIP3 signaling.

Autophagy is a self-consumption mechanism against adversities present within tumor microenvironment such as hypoxia and nutrition deprivation⁶. Here the present study proclaimed that α -MSH strikingly accelerated the LC3-II expression and GFP-LC3 puncta spots under hypoxic stress. Interestingly, inhibition of autophagy by

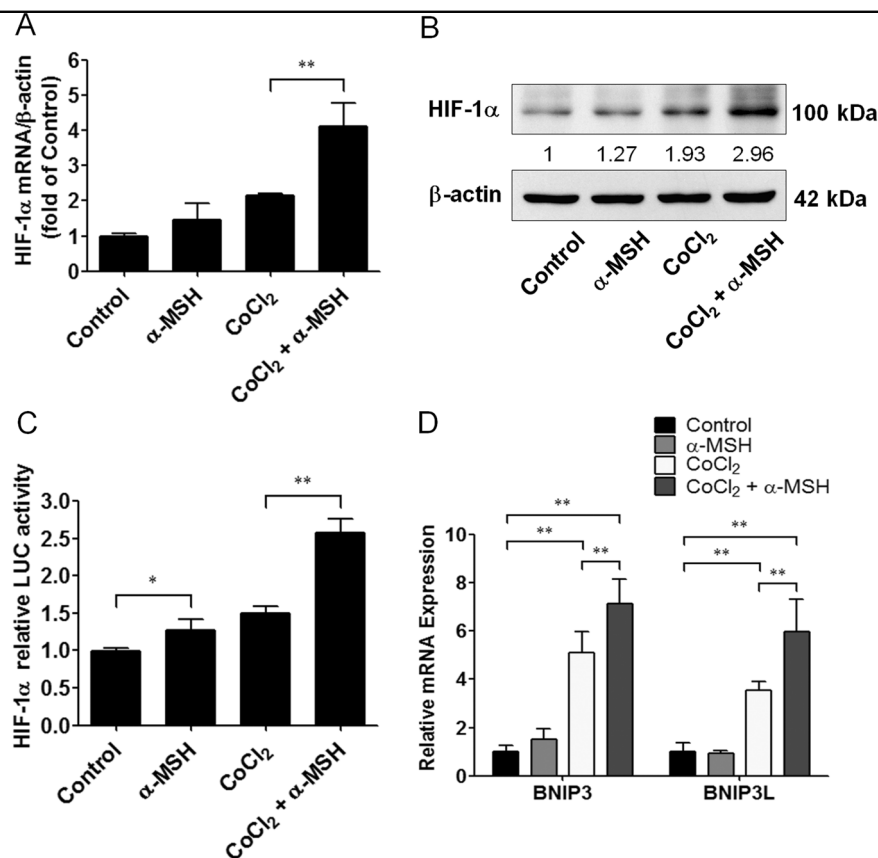


Fig. 6 Effect of α-MSH on HIF-1α expression and activity in B16-F10 melanoma cells during hypoxia. **a, b** α-MSH increased HIF-1α mRNA and protein expression levels during hypoxia. **c** Cells were transfected with luciferase reporter driven by a promoter region containing HIF-1α-specific binding sites before α-MSH treatment at the indicated time and concentration. The luciferase activities were measured immediately and expressed as means ± SD from triplicate experiments. **d** Relative mRNA expression levels were analyzed by real-time PCR. Data are expressed as fold change compared with control (means ± SD of triplicate experiments). * $p < 0.05$, ** $p < 0.01$. α-MSH elevated the Bcl-2 family gene expression levels by HIF-1α activation

3-MA or blocking ATG5 expression was enough to retard α-MSH-induced apoptosis, but autophagy-inducer rapamycin treatment contrarily increased the apoptosis of melanoma cells during hypoxia. Although autophagy is usually considered to protect tumor cells from apoptosis, these studies have implied that the induction of autophagy indeed participate in apoptotic process under some specific stress conditions^{32–34}. Especially, ATG5 protein is indicated to directly interact with apoptosis-related protein and silencing ATG5 can reduce drug-induced cell death^{35,36}. Therefore, our results suggested that the additional enhancement of autophagy contributed to α-MSH-induced cell death in B16-F10 melanoma cells during hypoxia.

Accumulation of ROS is considered as one of the important mediators of autophagy in response to several stress conditions⁵. Zhang and colleagues recently indicated that enhancement of autophagy by ROS stimuli accelerated cell apoptosis and growth inhibition of melanoma cells in vitro and in vivo³⁷. Similar to this notion, the present study has shown that POMC-induced

autophagy contributed to cell apoptosis in melanoma cells during hypoxia. In the meantime, we also found that mitochondrial morphology change and dysfunctions in Ad-POMC-infected or α-MSH-treated cells during hypoxia (data not shown). Additionally, our previous study has demonstrated that POMC-induced apoptosis was through ROS accumulation²⁹. Therefore, we guessed that POMC-induced autophagy might directly regulate by ROS accumulation but this needs further investigation.

Given that HIF-1α upregulation is frequently implicated in response to hypoxic stress and autophagic process, the present study showed that α-MSH significantly increased HIF-1α transcriptional activity and both protein and mRNA levels in B16-F10 melanoma cells during hypoxia, and HIF-1α-mediated Bcl-2 family genes (BNIP3 and BNIP3L) were also elevated by double stresses (α-MSH and hypoxia). This finding is consistent with previous report suggesting that hypoxia-induced autophagy is through HIF-1α-mediated autophagy genes' (BNIP3 and BNIP3L) expression³⁸. Moreover, our results further demonstrated that silencing HIF-1α by RNA interference

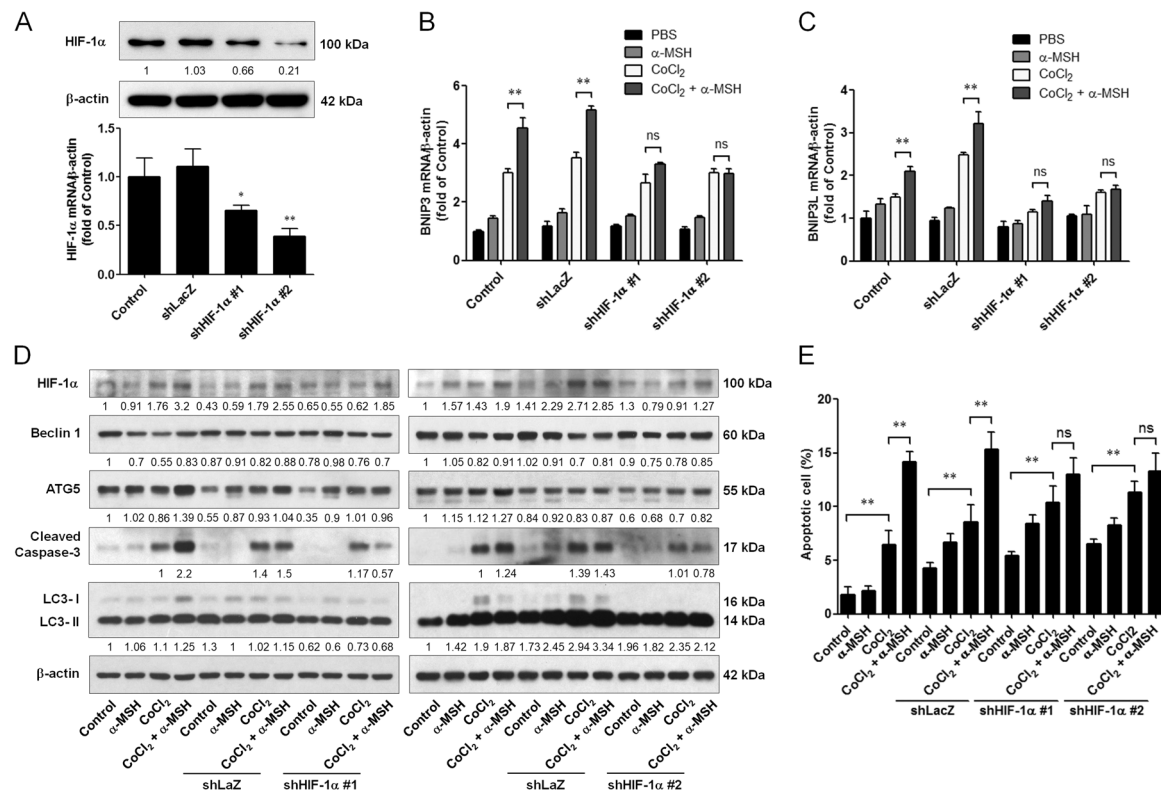


Fig. 7 Effect of HIF-1 α silencing on α -MSH-induced apoptosis in B16-F10 melanoma cells during hypoxia. **a** Cells were transfected with shLacZ or shHIF-1 α plasmids for 48 h before harvest. HIF-1 α shRNA reduced the basal HIF-1 α mRNA and protein expression levels. **b, c** Relative mRNA expression levels were analyzed by real-time PCR. Data are expressed as fold change compared with control (means \pm SD of triplicate experiments). **d** Cell lysates were analyzed by immunoblot using the indicated antibodies. β -Actin was used as an internal control for loading and transfer. **e** The population of apoptotic cells was analyzed by flow cytometry and qualified as mean \pm SD from triplicate experiments. * p < 0.05, ** p < 0.01. Knockdown of HIF-1 α diminished α -MSH-induced apoptosis in B16-F10 melanoma cells during hypoxia

abolished the α -MSH-stimulated autophagy genes' expression and eventually retarded α -MSH-induced apoptosis in melanoma cells during hypoxia. Therefore, we hypothesize that the induction of autophagy genes by HIF-1 α could contribute to α -MSH-induced apoptosis in B16-F10 melanoma cells during hypoxia as previously described^{32,39}.

In summary, the present study unveils that POMC gene therapy suppresses melanoma through activation of both autophagic and apoptotic signaling pathways in melanoma cells. Besides, combination therapy using α -MSH in conjunction with autophagy inducer such as rapamycin may facilitate a novel therapeutic strategy for melanoma control.

Materials and Methods

Cell cultures and reagents

Human MNT-1 melanoma cells were acquired as gift from Dr. Chung-Hsing Chang (Kaohsiung Medical University, Taiwan). Mouse (B16-F10) and human (A375 and A2058) melanoma cells were purchased from American Type Culture Collection (Manassas, VA, USA). These

cells were cultured in Dulbecco's modified Eagle's medium (Invitrogen; Carlsbad, CA, USA) containing 10% fetal bovine serum (Hyclone, Logan, UT, USA), 2 mM glutamine, 100 mg/ml streptomycin (Invitrogen; Carlsbad, CA, USA), and 100 U/ml penicillin at 37 °C in 5% CO₂ atmosphere. The following reagents were purchased from Sigma-Aldrich (St. Louis, MO, USA): 3-MA (M9281), rapamycin (R0395), CoCl₂ (60818), and β -actin (A5441). The following antibodies were purchased from Cell Signaling Technology (Danvers, MA, USA): Beclin1 (3738), LC3A/B (12741), ATG5 (12994), and Caspase-3 (9662). Antibody against HIF-1 α (NB100-479) was purchased from Novus (St Louis, MO, USA). Other antibodies were purchased from Santa Cruz Biotechnology (Santa Cruz, CA, USA): Bax (sc-7480) and Bcl-2 (sc-7382). The α -MSH peptide was purchased from BACHEM (Torrance, CA, USA).

Preparation of Ad vectors

Preparation of recombinant Ads containing POMC gene (Ad-POMC) or control GFP (Ad-GFP) were performed as previously described²⁴.

Flow cytometric analysis

The apoptosis of B16-F10 cells after gene delivery or α -MSH treatment was analyzed by flow cytometry as described previously²⁹. Briefly, cell aliquots were incubated with RNase A (10 μ g/ml) and propidium iodide (50 μ g/ml) for 30 min at 37 °C. DNA content of 10,000 events was analyzed using a FACS Caliber flow cytometer (Becton Dickinson Biosciences; San Jose, CA, USA) and the CELLQuest software.

Immunofluorescence staining of fixed tumor sections

After deparaffinization, the slides were blocked with 3% hydrogen peroxide for 10 min and subjected to antigen retrieval with microwave in 10 mM citrate buffer for 15 min. Then subsequently, the slides were blocked with a 5% (v/v) bovine serum albumin (BSA) and 0.1% (v/v) Triton X100 for 30 min and incubated with the indicated primary antibodies at 4 °C overnight. After a wash with phosphate buffer solution, the sections were incubated with Alexa Fluor-conjugated secondary antibody (Invitrogen; Carlsbad, CA, USA) for 1 h and subsequently counterstained with 4,6-diamidino-2-phenylindole for 10 min and viewed under a fluorescent microscope.

Confocal microscopy

Cells were grown on glass coverslips for 16 h. After gene delivery or peptide treatment, cells were stained with MitoTracker Orange CM-H₂TMRos (Molecular Probes Inc., M7511) for 15 min at 37 °C and then cells were fixed with 4% (v/v) paraformaldehyde for 5 min and permeabilized with phosphate-buffered saline containing 0.1% (v/v) Triton X-100 and 2% (v/v) BSA at room temperature for 5 min. Cells were then labeled with anti-Bax (Santa Cruz Inc; Santa Cruz, CA, USA) antibody for 30 min and with Alexa Fluor-conjugated goat anti-mouse antibody (Invitrogen; Carlsbad, CA, USA) for 30 min. Labeled cells were visualized with LSM510 (Carl Zeiss, Thornwood, NY, USA).

Autophagy analysis by GFP-LC3

Cells grown on glass coverslips were transfected with GFP-LC3 plasmid DNA (a gift from Dr. T. Yoshimori, Osaka University, Osaka, Japan) using Lipofectamine 3000 Reagent (Invitrogen; Carlsbad, CA, USA) based on the manufacturer's instructions for 24 h⁴⁰. After transfection, cells were incubated with α -MSH (10 nM) in the presence or absence of CoCl₂ (100 μ M) for another 24 h. The formation of GFP-LC3 punctate structures were visualized with LSM510 (Carl Zeiss, Thornwood, NY, USA).

Gene knockdown using shRNA

Various pLKO.1 plasmids to knockdown HIF-1 α , ATG5, and scramble control were purchased from

National RNAi Core Facility of Academia Sinica (Taipei, Taiwan). Briefly, cells were transiently transfected with 2 μ g of plasmids by Lipofectamine 3000 Reagent (Invitrogen; Carlsbad, CA, USA) according to manufacturer's instructions. After transfection for 24 h, cells were treated with α -MSH (10 nM) for 24 h and then incubated in the presence or absence of CoCl₂ (100 μ M) for another 24 h before harvest for the indicated assays.

HIF-1 α luciferase assay

Cells were co-transfected with HIF-1 α -driven luciferase (Stratagene, La Jolla, CA, USA) vector and the *Renilla reniformis* luciferase reporter vector (Promega, Madison, WI, USA) at a ratio of 1:1/10 using Lipofectamine 3000 Reagent (Invitrogen; Carlsbad, CA) for 4 h before being maintained with fresh medium for 24 h. Subsequently, cells were treated with α -MSH (10 nM) for 24 h and then incubated in the presence or absence of CoCl₂ (100 μ M) for another 24 h. The HIF-1 α -driven luciferase activities in cells were measured using a Dual-Light Kit (Promega, Madison, WI, USA) in Orion II microplate luminometer (Titertek Berthold; Pforzheim, Germany) and normalized with that of *R. reniformis* luciferase according to the manufacturer's instructions.

Western blot analysis

Cell lysates were prepared and the level of protein expression was measured as previously described²⁷. The PVDF membrane was blocked with 5% milk in TBS-T for 1 h and then incubated with specific primary antibodies and secondary antibodies conjugated with horseradish peroxidase (HRP; 1:10,000 dilutions in 5% milk) for 1 h, respectively. The signals on membrane were detected using chemiluminescent HRP substrate (Millipore Corporation; Billerica, MA, USA) and exposed to X-ray film for autoradiogram.

Quantitative real-time PCR

RNA was purified and quantitative real-time PCR was performed as previously described²⁹. The cDNA product was used for quantitative real-time PCR by the SYBR Green PCR master mix and the predesigned gene-specific probe and primer sets for mouse HIF-1 α (NM_010431.2), BNIP3 (NM_009760.4), and BNIP3L (NM_009761.3). Data were normalized to β -actin (NM_007393.3) and expressed as fold changes over that in the control experiments. The primer sequences were as follows: HIF-1 α forward primer (5'-ATG TGA CCA TGA GGA AAT GAG AGA A-3') and reverse primer (5'-CTG AGG TTG GTT ACT GTT GGT ATC A-3'); BNIP3 forward primer (5'-ACA CCA CAA GAT ACC AAC AGA G-3') and reverse primer (5'-TGT TTC TCA TGC TGA GAG TAG C-3'); BNIP3L forward primer (5'-GCC CTT CAC CAC AAG AAG AT-3') and reverse primer (5'-TTA

GAG ACG CAG CAC GTT TAG-3'); and β -actin forward primer (5'-GGA ATC CTG TGG CAT CCA T-3') and reverse primer (5'-GCT CAG GAG GAG CAA TGA T -3').

Statistical analysis

All data are expressed as the mean \pm standard deviation (SD). Statistical analysis was performed with one-way analysis of variance followed by Newman-Keuls post hoc or *t* test (for multiple comparisons) using Prism ver.5 (GraphPad Software, Inc., California, USA). A *P* value of <0.05 was regarded as statistically significant.

Acknowledgements

This work was supported in part by National Research Program for Biopharmaceuticals grants (MOST-105-2314-B-075B-002, MOST-105-2325-B-110-002), Kaohsiung Veterans General Hospital, Taiwan (VGHNSU104-003, VGHNSU105-001, and VGHNSU106-004), and National Sun Yat Sen University-Kaohsiung Medical University Joint Grant (105P-023).

Author details

¹Doctoral Degree Program in Marine Biotechnology, National Sun Yat-sen University, 70 Lien-Hai Road, Kaohsiung 80424, Taiwan. ²Doctoral Degree Program in Marine Biotechnology, Academia Sinica, 128 Academia Road, Section 2, Nankang, Taipei 11529, Taiwan. ³Institute of Chemistry, Academia Sinica, 128 Academia Road, Section 2, Nankang, Taipei 11529, Taiwan. ⁴Centre for Eye Research Australia, Royal Victorian Eye and Ear Hospital, East Melbourne, VIC, Australia. ⁵Ophthalmology, Department of Surgery, University of Melbourne, East Melbourne, VIC, Australia. ⁶Department of Dermatology, Kaohsiung Veterans General Hospital, Kaohsiung 813, Taiwan. ⁷Institute of Biomedical Science, National Sun Yat-sen University, Kaohsiung 804, Taiwan. ⁸Center for Neuroscience, National Sun Yat-sen University, Kaohsiung 804, Taiwan

Conflict of interest

The authors declare that they have no conflict of interest.

Publisher's note

Springer Nature remains neutral with regard to jurisdictional claims in published maps and institutional affiliations.

The online version of this article (<https://doi.org/10.1038/s41420-018-0070-5>) contains supplementary material, which is available to authorized users.

Received: 1 November 2017 Revised: 2 December 2017 Accepted: 13 December 2017

Published online: 10 July 2018

References

- Vaupel, P. & Mayer, A. Hypoxia in cancer: significance and impact on clinical outcome. *Cancer Metastasis Rev.* **26**, 225–239 (2007).
- Mazure, N. M. & Pouyssegur, J. Hypoxia-induced autophagy: cell death or cell survival? *Curr. Opin. Cell Biol.* **22**, 177–180 (2010).
- Papandreou, I. et al. Anoxia is necessary for tumor cell toxicity caused by a low-oxygen environment. *Cancer Res.* **65**, 3171–3178 (2005).
- Brunelle, J. K. et al. Loss of McI-1 protein and inhibition of electron transport chain together induce anoxic cell death. *Mol. Cell. Biol.* **27**, 1222–1235 (2007).
- Scherz-Shouval, R. & Elazar, Z. Regulation of autophagy by ROS: physiology and pathology. *Trends Biochem. Sci.* **36**, 30–38 (2011).
- Marino, G., Niso-Santano, M., Baehrecke, E. H. & Kroemer, G. Self-consumption: the interplay of autophagy and apoptosis. *Nat. Rev. Mol. Cell Biol.* **15**, 81–94 (2014).
- Li, M., Tan, J., Miao, Y., Lei, P. & Zhang, Q. The dual role of autophagy under hypoxia-involvement of interaction between autophagy and apoptosis. *Apoptosis* **20**, 769–777 (2015).
- Choi, A. M., Ryter, S. W. & Levine, B. Autophagy in human health and disease. *N. Engl. J. Med.* **368**, 651–662 (2013).
- Levine, B., Mizushima, N. & Virgin, H. W. Autophagy in immunity and inflammation. *Nature* **469**, 323–335 (2011).
- Levine, B. & Kroemer, G. Autophagy in the pathogenesis of disease. *Cell* **132**, 27–42 (2008).
- White, E., Karp, C., Strohecker, A. M., Guo, Y. & Mathew, R. Role of autophagy in suppression of inflammation and cancer. *Curr. Opin. Cell Biol.* **22**, 212–217 (2010).
- Munz, C. Enhancing immunity through autophagy. *Annu. Rev. Immunol.* **27**, 423–449 (2009).
- White, E. Deconvoluting the context-dependent role for autophagy in cancer. *Nat. Rev. Cancer* **12**, 401–410 (2012).
- Armstrong, J. L. et al. Exploiting cannabinoid-induced cytotoxic autophagy to drive melanoma cell death. *J. Invest. Dermatol.* **135**, 1629–1637 (2015).
- Yoo, B. H. et al. Hypoxia-induced downregulation of autophagy mediator Beclin 1 reduces the susceptibility of malignant intestinal epithelial cells to hypoxia-dependent apoptosis. *Autophagy* **5**, 1166–1179 (2009).
- Noman, M. Z. et al. Blocking hypoxia-induced autophagy in tumors restores cytotoxic T-cell activity and promotes regression. *Cancer Res.* **71**, 5976–5986 (2011).
- Tracy, K. et al. BNIP3 is an RB/E2F target gene required for hypoxia-induced autophagy. *Mol. Cell. Biol.* **27**, 6229–6242 (2007).
- Greijer, A. E. & van der Wall, E. The role of hypoxia inducible factor 1 (HIF-1) in hypoxia induced apoptosis. *J. Clin. Pathol.* **57**, 1009–1014 (2004).
- Kubli, D. A. & Gustafsson, A. B. Mitochondria and mitophagy: the yin and yang of cell death control. *Circ. Res.* **111**, 1208–1221 (2012).
- Raffin-Sanson, M. L., de Keyser, Y. & Bertagna, X. Proopiomelanocortin, a polypeptide precursor with multiple functions: from physiology to pathological conditions. *Eur. J. Endocrinol.* **149**, 79–90 (2003).
- Garfield, A. S., Lam, D. D., Marston, O. J., Przydzial, M. J. & Heisler, L. K. Role of central melanocortin pathways in energy homeostasis. *Trends Endocrinol. Metab.* **20**, 203–215 (2009).
- Hegadoren, K. M., O'Donnell, T., Lanius, R., Coupland, N. J. & Lacaze-Masmonet, N. The role of beta-endorphin in the pathophysiology of major depression. *Neuropeptides* **43**, 341–353 (2009).
- Rousseau, K. et al. Proopiomelanocortin (POMC), the ACTH/melanocortin precursor, is secreted by human epidermal keratinocytes and melanocytes and stimulates melanogenesis. *FASEB J.* **21**, 1844–1856 (2007).
- Liu, G. S. et al. Gene transfer of pro-opiomelanocortin prohormone suppressed the growth and metastasis of melanoma: involvement of alpha-melanocyte-stimulating hormone-mediated inhibition of the nuclear factor kappaB/cyclooxygenase-2 pathway. *Mol. Pharmacol.* **69**, 440–451 (2006).
- Tsai, H. E. et al. Downregulation of hepatoma-derived growth factor contributes to retarded lung metastasis via inhibition of epithelial-mesenchymal transition by systemic POMC gene delivery in melanoma. *Mol. Cancer Ther.* **12**, 1016–1025 (2013).
- Tsai, H. E. et al. Pro-opiomelanocortin gene delivery suppresses the growth of established Lewis lung carcinoma through a melanocortin-1 receptor-independent pathway. *J. Gene Med.* **14**, 44–53 (2012).
- Liu, G. S. et al. Systemic pro-opiomelanocortin expression induces melanogenic differentiation and inhibits tumor angiogenesis in established mouse melanoma. *Hum. Gene Ther.* **22**, 325–335 (2011).
- Weng, W. T. et al. alpha-Melanocyte-stimulating hormone inhibits angiogenesis through attenuation of VEGF/VEGFR2 signaling pathway. *Biochim. Biophys. Acta* **1840**, 1850–1860 (2014).
- Liu, G. S. et al. Proopiomelanocortin gene delivery induces apoptosis in melanoma through NADPH oxidase 4-mediated ROS generation. *Free Radic. Biol. Med.* **70**, 14–22 (2014).
- Kuma, A. et al. The role of autophagy during the early neonatal starvation period. *Nature* **432**, 1032–1036 (2004).
- Noman, M. Z., Janji, B., Berchem, G., Mami-Chouaib, F. & Chouaib, S. Hypoxia-induced autophagy: a new player in cancer immunotherapy? *Autophagy* **8**, 704–706 (2012).
- Song, Z. C., Zhou, W., Shu, R. & Ni, J. Hypoxia induces apoptosis and autophagic cell death in human periodontal ligament cells through HIF-1alpha pathway. *Cell Prolif.* **45**, 239–248 (2012).

33. B'Chir, W. et al. Dual role for CHOP in the crosstalk between autophagy and apoptosis to determine cell fate in response to amino acid deprivation. *Cell. Signal.* **26**, 1385–1391 (2014).
34. Tomic, T. et al. Metformin inhibits melanoma development through autophagy and apoptosis mechanisms. *Cell Death Dis.* **2**, e199 (2011).
35. Pyo, J. O. et al. Essential roles of Atg5 and FADD in autophagic cell death: dissection of autophagic cell death into vacuole formation and cell death. *J. Biol. Chem.* **280**, 20722–20729 (2005).
36. Yousefi, S. et al. Calpain-mediated cleavage of Atg5 switches autophagy to apoptosis. *Nat. Cell Biol.* **8**, 1124–1132 (2006).
37. Xie, J. et al. A novel ECG analog 4-(S)-(2,4,6-trimethylthiobenzyl)-epigallocatechin gallate selectively induces apoptosis of B16-F10 melanoma via activation of autophagy and ROS. *Sci. Rep.* **7**, 42194 (2017).
38. Bellot, G. et al. Hypoxia-induced autophagy is mediated through hypoxia-inducible factor induction of BNIP3 and BNIP3L via their BH3 domains. *Mol. Cell. Biol.* **29**, 2570–2581 (2009).
39. Wang, X., Li, J., Wu, D., Bu, X. & Qiao, Y. Hypoxia promotes apoptosis of neuronal cells through hypoxia-inducible factor-1alpha-microRNA-204-B-cell lymphoma-2 pathway. *Exp. Biol. Med. (Maywood)* **241**, 177–183 (2016).
40. Kabeya, Y. et al. LC3, a mammalian homologue of yeast Apg8p, is localized in autophagosome membranes after processing. *EMBO J.* **19**, 5720–5728 (2000).